Unsteady loading in a tidal array due to simulated turbulent onset flow

Author accepted manuscript of:
Mullings, H., Stallard, T. (2018) Unsteady Loading in a tidal array due to simulated turbulent onset flow. Paper Number 84. Proceedings of the 3rd International Conference on Renewable Energies Offshore. Lisbon, Portugal, 8-10 October 2018.

Unsteady loading in a tidal array due to simulated turbulent onset flow

H. Mullings & T. Stallard
School of Mechanical, Aerospace and Civil Engineering, Faculty of Science and Engineering,
The University of Manchester, M13 9PL, UK

Understanding of operational and environmental loads is necessary for fatigue design of tidal turbines. A von Kármán spectral method and a Synthetic Eddy Method are analysed for prediction of unsteady loads on a horizontal axis turbine. The blade load spectrum by the von Kármán method is in reasonable agreement with existing experimental measurements for frequencies less than the fourth harmonic of the rotor frequency but over-predicts at higher frequencies. The Synthetic Eddy Method over-predicts at low frequencies but under-predicts at higher frequencies. However, both methods provide reasonable prediction of the damage equivalent load at the blade passing frequency. This approach is used to evaluate damage equivalent loads due to in-wake and in-array operation. It is shown that the tip-speed-ratio of each turbine in the array can be selected to standardize damage equivalent load across the turbines and, for the particular turbine specification considered, this also increases power slightly compared to an array with all turbines operating at the same point.

1 INTRODUCTION

Tidal stream turbines deployed in narrow channels and straits are receiving increasing interest for renewable power generation. It is expected that such devices would be installed in arrays, e.g. Meygen Project in the Pentland Firth, akin to wind farms, to extract energy at sufficient scale to provide a valued contribution to electricity supply whilst recognizing environmental constraints. The design of each turbine is governed by fatigue considerations and so it is essential to understand through-life cyclic loading, particularly for in-array operation.

Key issues affecting cyclic loading are the occurrence and characteristics of the environmental conditions onset to the turbine at a given site. Key phenomena include waves, onset shear and turbulence (DNV-GL, 2015). These factors and their influence on the reliability of components in a single turbine have received some attention in the literature. McCann (2007), Galloway (2013) and Togneri et al. (2017) focus on loading experienced by blades. A study by the authors (Mullings et al., 2017) examined the variation of thrust and damage equivalent loads on the rotor, characterizing unsteady load spectra using experimental data scaled to turbulence characteristics of a representative site through a tidal cycle. For a given location, the onset conditions to a turbine will differ for a turbine operating within an array rather than in isolation, e.g. Olczak et al. (2013) and Vogel and Willden (2015).

This study addresses development of a simplified approach to modelling the load spectra for a turbine, to represent loading due to turbulence and onset shear, and application of this to assess load variation for isolated turbines and turbines within simple multi-row arrays. Loading due to turbulence is assessed using alternative onset turbulence synthesis methods, shown in Burton et al. (2011) and Jarrin et al. (2006). The variations in loading due to the different onset flow fields are compared to the experimental dataset of Payne et al. (2017b). The influence of onset flow due to upstream wakes is also assessed. For turbines subject to upstream turbine wakes, operating points are identified to attain a similar design life for each turbine across the array, here based on the damage equivalent load.

Section 2 provides an explanation of the methods used within this paper for assessment of reliability and the generation of onset velocity fields. Evaluation of the load predictions relative to measurements for a single three-bladed turbine is presented in Section 3. In Section 4 the approach is employed to investigate the influence of in-wake operation and in-array operation on damage equivalent loads prior to some concluding remarks.

Author accepted manuscript of:
Mullings, H., Stallard, T. (2018) Unsteady Loading in a tidal array due to simulated turbulent onset flow. Paper Number 84. Proceedings of the 3rd International Conference on Renewable Energies Offshore. Lisbon, Portugal, 8-10 October 2018.

2 METHOD

2.1 Determining Load Cycles

Following a similar approach to McCann et al. (2006), reliability is assessed through Damage Equivalent Loads (DEL):

$$DEL = \left(\frac{\sum_i n_i L_i^m}{fT}\right)^{\frac{1}{m}} \quad (1)$$

Where L_i is the load at bin 'i', m is a material property given by the slope of the S-N curve for the material, T is the length of time for operation, f is the repetition frequency, n_i is the number of cycles at a given load. Taking a time history of force, such as thrust or root bending moment, as input the magnitude of each cycle is binned using Rainflow Cyclic counting (see Downing & Socie, 1982).

Cyclic loading can be considered as deterministic, predominantly due to rotation of the blade through shear or in proximity to a structure, as well as wave-induced kinematics, and stochastic, due to turbulence. Prediction methods include Blade Element Momentum Theory (BEM) models, Masters et al. (2011) and Computational Fluid Dynamics (CFD), such as Ouro et al. (2017), Mason-Jones et al. (2013) and Ahmed et al. (2017). A CFD model with an unsteady inflow with coherent turbulence structure such as the model used in Ahmed et al. (2017), can provide insight to fluctuating flow and loads at the blade scale. However fully resolved cases require considerable computational resources. BEM models are computationally efficient relative to CFD although rely on 2D airfoil performance data in steady flow so do not fully capture the effect of unsteady onset flow on blade performance and simplified approaches are required to represent the effect of fixed supports on blade loading.

The focus of this study is to assess load variation using a consistent method suited to rapid application to a wide range of environmental onset conditions including in-array onset conditions. As such a simple approach is taken, in which a synthesised unsteady velocity field is generated and the streamwise component reduced by the axial induction factor to define streamwise flow at the rotor plane and, hence relative velocity to each blade segment. The approach is evaluated using flow characteristics and turbine loading from experiments undertaken at the IFREMER flume in Boulogne-Sur-Mer, Payne et al. (2017a), with mean flow velocity 0.8 m/s and turbine diameter 1.2 m. Time-varying thrust, and for some cases blade root bending, were measured for onset turbulence of 3% and 12%.

2.2 Turbulence characteristics

Experimental studies have shown that although onset turbulence has limited effect on mean power and thrust, the instantaneous loading and hence power are both significantly affected by the characteristics of the onset flow, e.g. Chamorro et al. (2013) and Blackmore et al. (2016). Mycek et al. (2014) and Milne et al. (2010) conclude that turbulence intensity is the dominant factor influencing fatigue of blades, as increasing values were observed to cause dramatic increase of load fluctuations. Secondary factors include parameters such as the integral lengthscale that represents the proportion of turbulent energy, through the eddy size, which effects the performance of the turbine, as investigated in Blackmore et al. (2016).

2.3 Simulation of Onset Turbulence

Incorporation of a time-varying velocity field with defined turbulence parameters as inflow to numerical analysis such as BEM or CFD may be conducted using either a spectral or synthetic model. The spectral model used here is the von Kármán model as this allows specification of integral length-scales for designers, as discussed in the DNV-GL standard on Tidal Turbines, DNV-GL (2015). The flow speed time-histories are created using specific auto-spectral density and spatial cross-correlation coherence and here a velocity field of this form was generated using DNV GL Tidal Bladed, (Bossanyi, 2003). The synthetic turbulence is generated with the synthetic eddy method developed by Jarrin et al. (2008). A code developed by Polleto (2013) was used to specify length-scale, turbulence intensity and number of eddies.

Author accepted manuscript of:
Mullings, H., Stallard, T. (2018) Unsteady Loading in a tidal array due to simulated turbulent onset flow. Paper Number 84. Proceedings of the 3rd International Conference on Renewable Energies Offshore. Lisbon, Portugal, 8-10 October 2018.

Table 1. Comparison of Length-scale between turbulence generation methods and Experiment

Inflow method	Lengthscale (m)	% Difference
Experimental	0.6	-
von Kármán	0.5381	10%
Synthetic Eddy Method	0.4791	20%

Table 1 shows a comparison between the target length-scale and recovered integral length-scale obtained by auto-correlation method at the centre of the domain. In both cases the sampling frequency was 307 Hz. This frequency corresponds to 1 sample point per 1.5 degree rotation at TSR of approximately 5.89 (8 rad/s). These conditions represent the onset flow in the dataset of (Payne et al. 2017a) for a low turbulence case (3%) and this is used for evaluation of load prediction in Section 3.

The onset flow velocity spectrum for each method is compared to the measurements reported in the experimental low turbulence case, Figure 1. It is clear that the overall magnitude in the low frequency range (f < 1 Hz) is very similar for all cases. However in the mid frequency range (1 Hz < f < 20 Hz) the von Kármán spectra continues with a similar magnitude and gradient but the SEM has a significant decrease in magnitude at approximately 2 Hz. Note that this method was originally proposed to develop only large-scale coherent structures at the inflow to a CFD simulation, rather than to represent all scales of turbulent structure. For such applications the breakdown of coherent structures results in finer scale fluctuations, or transported kinetic energy across the high frequency range. Recent developments by Carlier et al. (2015) show how Gaussian distribution of eddy sizes can be used to represent a wider range of energy-carrying scales, partly addressing this limitation of the SEM approach.

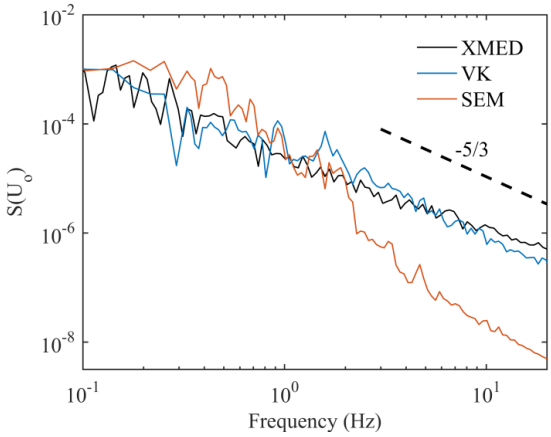

Figure 1: Power Spectra for the Onset Flow from the experimental data, XMED (Black), the von Kármán (Blue) and Synthetic Eddy Method (Orange)

2.4 Blade Scale Flow

To determine load spectra for a synthesized case, time varying load is required. The major contribution to loading is the incremental thrust force in the streamwise direction, evaluated for each time step:

$$\partial F_T = \partial L \sin(\varphi) - \partial D \cos(\varphi) \quad (4)$$

where ∂F_T is the variation of thrust on each element over time, ∂L is the variation in lift force, ∂D is the variation in drag force and φ is the inflow angle to each blade element relative to the rotor plane. This is calculated based upon the time varying velocity, which is extracted at the instantaneous position of a blade element within the velocity field. The position of the blade at each time step is determined by the angular frequency and dictates the tip-speed-ratio of the turbine with loading assessed over a range of tip speed ratio (TSR). Both the relative velocity and angle of flow to the blade are defined by the velocities extracted from the turbulent velocity field by:

Author accepted manuscript of:
Mullings, H., Stallard, T. (2018) Unsteady Loading in a tidal array due to simulated turbulent onset flow. Paper Number 84. Proceedings of the 3rd International Conference on Renewable Energies Offshore. Lisbon, Portugal, 8-10 October 2018.

$$U_{rel} = \sqrt{U_{x,D}^2 + (\Omega r - U_\Theta)^2} \quad (2)$$

$$\varphi = sin^{-1}\left(U_{x,D}/U_{rel}\right) \quad (3)$$

Herein, the streamwise velocity at the disc $U_{x,D}$ is taken as the disc velocity $U_d = U_\infty(1-a)$, where a is taken as the axial induction factor at the segment radius, a reduction from the ambient velocity U_∞. The azimuthal velocity is the resolved component of U_y and U_z at the blade position, with the inclusion of the radially varying tangential induction factor, $U_\Theta = (U_y^2 + U_z^2)^{1/2} + \Omega r a'$. The radial variation of both induction factors is determined through a steady BEMT calculation. Both the relative velocity and corresponding angle of attack fluctuate with time, providing an example of the type of influence the turbulence can have on the loading cycles at one quasi-steady point.

2.4.1 Tower Shadow

The effect of tower shadow is briefly investigated to assess influence on unsteady loads relative to shear. The onset flow speeds are modified by Equations 4-5, where U_y becomes V_y and $U_{x,D}$ become $V_{x,\mathrm{D}}$ whilst the blades are in the lower half of the rotor's swept area only:

$$V_y = U_\infty \left(\frac{r_t^2}{d_{rs}^2}\right) \sin(2\varphi) \quad (4)$$

$$V_x = U_\infty \left(1 - \left(\frac{r_t^2}{d_{rs}^2}\right) \cos(2\varphi)\right) \quad (5)$$

where d_{rs} is the distance of each blade segment to the tower centre (504 mm), r_t is the tower radius (50 mm), φ is the angle between the blade segment and the positive stream-wise direction, x_{rt} is the distance between the rotor and tower centre. Typical overhang ratios for wind turbines of 0.2 to 0.33 affect the thrust by between 4 to 8% (Smilden et al. 2016). For this case the experimental tidal turbine has a smaller ratio (0.1), and hence it would be expected to have a smaller variation of thrust and potentially less impact on the magnitude of loads at the tower passing frequency.

2.4.2 Shear Profile

In a realistic tidal flow a vertical shear profile is present due to the boundary layer caused by the sea-bed. Such profiles may be approximated by either a logarithmic profile or a power law profile (Lewis et al. 2015). Here a power law profile is used where the onset flow is proportional to $z^\propto$, where z is vertical ordinate and $\propto$ is a function of roughness and termed the power law index. This can be determined from full scale measurements, as seen in the work by Togneri et al. 2011, with variation often observed over a tidal cycle.

3 SINGLE TURBINE BLADE LOADING

To assess load predictions using the methods of Section 2, the spectrum of blade root bending moments and, subsequently, of thrust are compared to lab scale results. Firstly, blade loading is examined as the segmental thrust force multiplied by the distance along the radius and compared to the experimental measurement of root bending moment. In Figure 2 the energy spectra of the root bending moment is shown for one blade for each onset flow method and the experimental case.

In each case the frequencies have been normalised by the rotor frequency, as this is the dominant frequency of loading on a single blade due to rotation upstream of the fixed tower and through a sheared velocity profile. In the low frequency range (f/f_0 < 1 Hz) the von Kármán case has a similar magnitude to the measurements of Payne et al. (2017b), with the SEM having slightly more energy. In the mid frequency range (1 < f/f_0 < 30) there are peaks as expected from the experimental case at multiples of the tower passing frequency, these are due to the influence of tower shadow and any shear effects within the onset flow. As expected these peaks are not visible using either turbulent flow alone and so these loads are superposed in Section 2.4.

The magnitude of load fluctuations due to SEM is higher than the experimental results for f/f_0 < 4 and for higher frequencies the energy reduces with a steeper gradient. In contrast the von Kármán approach has a similar magnitude to the experiments for frequencies up to f/f_0 = 4. However, the magnitude and gradient is slightly higher than the experimental results in the higher frequency range (4 < f/f_0 < 30). Over this range the

loading may be affected by distortion of the onset turbulence and blade generated turbulence (e.g. Ahmed et al. 2017). The frequency area of interest for the influence on loading in this section is the low and mid-frequency ranges. Various cases are shown here to assess the influence of the tower shadow, vertical shear and transverse shear on the magnitude of the energy spectra for the blade root bending and resultant damage equivalent load.

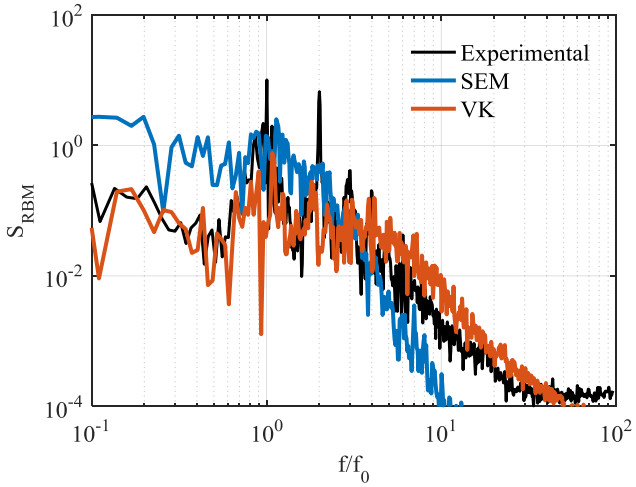

Figure 2: Power Spectra for the Bending root moment for one blade, from the experimental data (black), the von Kármán (Orange) and Synthetic Eddy Method (Blue).

3.1 Load Cycles

Rainflow cycle counting is applied to the predicted and measured force time histories using the method of Section 2.1. This determines the total full and half cycles at pre-defined binned amplitudes, in the case of root bending moment the binned amplitudes are of 0.2 Nm. Based upon the time history of root bending moment the load cycles for the inclusion of the onset flow are determined. Table 2 includes the mean load magnitude and maximum cyclic magnitude of the root bending moment for the experimental case and each generation method.

Table 2. Load cycles of root bending moment by alternative inflow generation methods and from experimental data of Payne et al. (2017a)

Inflow method	Number of cycles	Magnitude of Cyclic Load (Nm) Mean	Maximum
Experimental	4301	40.3	5.05
von Kármán	3496	39.7	4.02
SEM	203	39.7	6.57

The maximum cyclic amplitudes differ for both generation methods, with the SEM case having a larger average cyclic than both the experimental and von Karman, this follows the observations in the lower frequency range of Figure 1, the larger magnitude for the SEM.

3.2 Influence of Onset Shear and Tower Shadow

The addition of a shear profile on to the load spectra shear generates a peak at the tower passing frequency (e.g. Figure 3), and a secondary peak is also visible at the first harmonic of this frequency. The magnitude of the peak at the rotor frequency for two vertical shear cases has been compared in Table 3. For both turbulence inflow generation methods the load amplitude at the rotor frequency is similar (within 1%) although greater than for the experiments as the shear across the rotor plane is slightly weaker than the applied profiles. Consideration of the disc velocity instead of the onset velocity only reduces the magnitude of mean and unsteady forces on the blade.

Author accepted manuscript of:
Mullings, H., Stallard, T. (2018) Unsteady Loading in a tidal array due to simulated turbulent onset flow. Paper Number 84. Proceedings of the 3rd International Conference on Renewable Energies Offshore. Lisbon, Portugal, 8-10 October 2018.

Table 3. Peak magnitude of load at rotor frequency

Inflow method	Peak Magnitude (Nm)	
	$1/7^{th}$	$1/20^{th}$
Experimental	-	14.09 -
von Kármán	222.7	28.04
Synthetic Eddy Method	221.9	29.15

Based upon the observed variation of velocity in the experiments a transverse shear profile has been included, as a linear variation across the rotor diameter. The load amplitude at the rotor frequency is within 2% of the experiments for ±2.5% variation of velocity across the rotor plane. Inclusion of the tower shadow model causes further increase in the peak loading at the rotor frequency for both onset flow methods but with smaller amplitude than the shear cases of Table 3. This could be due to the relatively small ratio between rotor overhang and tower diameter. However, regardless of the low impact on the non-shear case, the influence of the tower shadow, as well as axial induction and transverse shear should be determined.

3.3 Combined Influence

An example of the load spectrum by superposition of the effects of shear, axial induction and tower shadow with the loads from the turbulent velocity field is shown in Figure 3. For transverse shear and tower shadow the peak magnitude at rotor frequency are within 28% for the SEM case which is an improvement over the transverse shear only case. In general the experimental spectra is predicted with reasonable accuracy with the von Kármán method but with over-prediction for $f > 10f_0$. In contrast the SEM approach over-predicts at lower frequencies. Over the range f/f_0 = 0.1 to 1 which is partly associated with turbulent flow and partly with shear, the integral of the spectrum is within 5% for the von Kármán case but over-predicted by a factor of seven with the SEM model. However, despite the difference of spectra shape, the integral of each spectrum across the whole frequency range is within 1.6%.

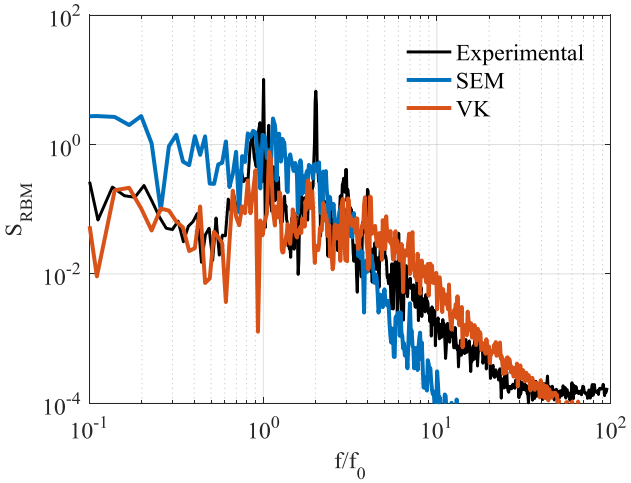

Figure 3: Power Spectra of the blade root bending moment with radially varying axial and tangential induction factors, linear variation of streamwise velocity across the rotor plane and tower shadow model applied for both generation methods. Experimental data (Black), the von Kármán (Orange) and Synthetic Eddy Method (Blue).

3.4 Damage Equivalent Loads

Damage equivalent loads are determined using a statistical method, shown in Equation 1. They are affected by the number of load cycles in the sample time. Herein the magnitude of a damage equivalent load is considered at a prescribed frequency, the rotor frequency f_0 for the blade loading and $3f_0$ for the rotor loading. This approach is employed for direct comparison between the two onset flow generation methods and to facilitate comparison to deterministic loads at these frequencies such as due to shear and tower shadow. As specific

material properties are not available, such as an S-N curve, for the blades of this device, the approach of Freebury and Musial (2000) is adopted. This employs a parameter 'm' to characterise the gradient of the S-N curve. For this analysis *m=10* is used as this specifies the use of a semi-flexible material such as glass fibre, and *m= 4* for steel. The damage equivalent loads are calculated for the various loading cases and shown in Figure 4. The results from each generation method are also given both with and without the predefined frequency.

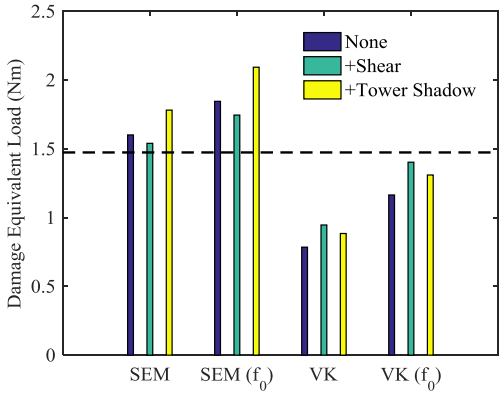

Figure 4: Magnitudes of DEL for an individual blade, for each generation method, with and without the imposed repetition frequency of f_0, with the DEL from the experimental case with imposed frequency shown as the dashed line.

Using the imposed repetition frequency the DEL is shown to increase for the blade for both generation methods. For the von Karman case the increase is a consistent 48%, however for the SEM case the increase is only between 15-17%. For the SEM case the imposed repetition frequency has less effect on the loads since the frequency based on load cycles would be similar, within a factor of 5, whereas the von Karman is a factor of 50 different. These variations are due to the reduction in magnitude of the high frequency cycles for the SEM case. Overall the von Kármán approach with imposed frequency produces DEL closest to the experimental case.

Including the tower shadow increases the DEL for both onset flows. A larger increase is found using the repetition frequency as the load due to the shear has greatest influence at the same frequency. A decrease of damage equivalent loads is shown with the addition of the transverse and vertical shear for the SEM case this is expected for the RBM as the larger magnitude low frequency fluctuations are more dominant in this case. To determine the effect on the entire rotor the thrust force on three blades rotating through the flow field is considered. The damage equivalent load for the experimental case is 0.68 N. This is about 30% larger than the loads determined through the use of the thrust on 3 blades, partly due to assumption of uniform disc velocity and neglecting the hub.

4 IN-ARRAY TURBINE LOADING

The previous sections address loading of a single turbine. In practice to maximize the potential of the relatively small geographic regions in which flow speeds are expected to be suitable for tidal stream systems, arrays of turbines are likely to be used. Turbines may thus be subject to transverse shear due to variation of onset flow along a fence, Cooke et al. (2015) or subject to onset flow due to the wakes of upstream turbines, e.g. Mycek et al. (2014). Two array configurations are considered with transverse profiles of the mean velocity of the wake defined by a Gaussian self-similar profile (Stallard et al. 2015). Here the focus is on the influence of transverse shear for distances of eight diameters downstream. For such positions turbulence is approximately constant across the width of the wake (Stallard et al. 2013), and fluctuating velocity at the downstream rotor is here approximated as an onset turbulent flow field using the SEM and von Kármán methods. This neglects the expected elevated value of turbulence intensity and spatial variation of turbulence across the swept area both of which would be of increasing influence with reducing downstream distance. Firstly, two turbines are considered, with a downstream turbine at 8 diameters downstream, either in-line or staggered by 0.5 diameters. Secondly a small array comprising of a row of four turbines 4 and 8 diameters downstream of a row of three

turbines, following the layouts in Olczak et al. (2016). The onset flow to the front row of turbines is approximated by a transverse shear profile with induction included and this is superposed with the mean wakes of the turbines of the first row defined by superposition of the velocity deficit.

4.1 In-wake operation

The amplitude and number of cycles of rotor thrust differ between the three rotor positions. For the von Kármán generation method, the total number of cycles reduces for both the in-line and offset case, but they remain within 15% of the isolated turbine shear case. For the SEM case the total number of cycles decreases by a maximum of 58% for the offset case and 22% for the inline. The inclusion of the transverse wake profile causes the number of cycles within the higher amplitude range to decrease when the turbine is directly in-line and causes the amplitude to increase for the offset case. This is expected due to the higher transverse shear experienced by the offset turbine within the shoulder of the Gaussian wake.

The resulting DEL have been determined over a range of operating points, TSR values of 3.92 to 7.12, for each rotor position and onset flow generation method, this is shown in Figure 5.

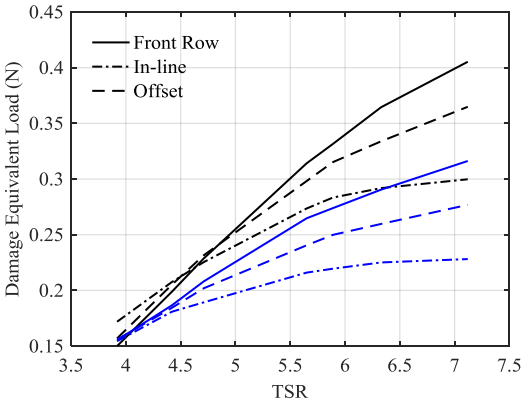

Figure 5: Variation in DEL magnitude with turbine position and operating point (TSR), SEM generation (Black), von Kármán (Blue)

For both generation methods the DEL increase with increasing TSR. With no transverse wake shear applied the DEL are consistently higher for the SEM generation case, with the SEM magnitude up to 31% greater than the von Karman. Regardless of magnitude the inclusion of the transverse shear for the offset wake causes a maximum reduction of 12% for the von Kármán and 10% for the SEM. The in-line wake causes a maximum decrease of 28% for the von Kármán and 26% for the SEM. For the von Karman case the front row turbine has consistently greater DELs than the downstream turbines. However for the SEM case the front row turbine only has greater DELs from approximately 4.75 TSR. This crossover point could be caused by the coherency of the structures within the SEM inflow model being more dominant at the lower rotational frequency.

For maximum power generation from an array an operating strategy would be for all turbines to operate at close to optimum power coefficient and hence similar TSR. As seen this would result in up to 88% variation of damage equivalent load between an upstream and downstream turbine depending on relative position. Optimum power coefficient is not always feasible. It may be desirable to select operating points with a view to similar operating life of key components. If on the first upstream turbine a TSR of 5 is chosen, an in-line turbine operating with TSR of 6.5 and an offset turbine operating with TSR of 5.5 would experience similar DEL magnitude. For this turbine, these TSRs when applied to the experimental C_P(TSR) curve, would lead to a 9% increase in C_P for the in-line case and a 7% increase for the offset case. In terms of overall power, based on C_P and the disc-averaged velocity cubed, there is a 4.1% increase in the offset position over the inline. The extent of the change of TSR required to attain similar DEL per turbine and the consequent change of power output would be turbine specific.

Author accepted manuscript of:
Mullings, H., Stallard, T. (2018) Unsteady Loading in a tidal array due to simulated turbulent onset flow. Paper Number 84. Proceedings of the 3rd International Conference on Renewable Energies Offshore. Lisbon, Portugal, 8-10 October 2018.

4.2 In-array operation

For the multi-row array case, the combined wake of the upstream rows is modelled with the approach of Stansby and Stallard (2016) with wakes superposed relative to a bypass flow the value of which is defined to maintain mass-flux at each section of the channel. Relative to an isolated rotor, the rotor averaged velocity (U_{DA}) and velocity squared, as a proxy for thrust force, for the second row of turbines is in reasonable agreement with the experimental and RANS-BEM data of Olczak et al. (2016), Figure 6.

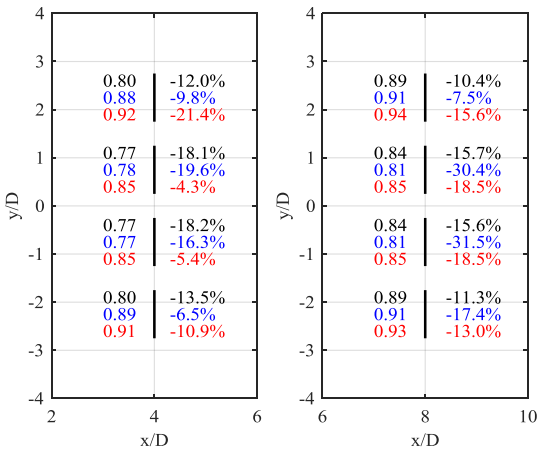

Figure 6: Left: variation of U_{DA}, Right: variation in equivalent mean force from row 1; SEM Results (Black), Olczak et al. (2016): Experimental (Blue), RANS-BEM (Red).

The variation of DEL magnitude within a three-row array is shown in Figure 7. The DEL across row 2 and row 3 decrease as the number of cycles increase, with the transverse shear of the wake. The overall maximum loads also reduce with downstream position. To operate an array where the rotors in different positions would experience similar damage equivalent loads the operating point of each turbine, the TSR, can be adjusted. For this purpose the DELs have been calculated on the second and third rows for a range of TSRs. In this case, using a TSR of 4.5 for the three rotors on the front, the TSR on the second row the TSR should vary between 5.2 and 5.9, as shown with the left-hand text on Figure 7. Higher TSR are required on the third row. For the thrust and power curve of the turbine considered, these changes of TSR result in an 8.7% increase in power over using the constant TSR of 4.5 on row 2 and 8.1% increase in power relative to application of TSR of 4.5 to all turbines. This is based on the measured C_P(TSR) reported by Payne et al. (2017a), for which the peak C_P is at TSR of 6.1, hence the increase in power observed from baseline case of TSR of 4.5. The extent to which this approach may be applied to minimise variation of load between turbines and to which operating parameters could be adjusted would differ with turbine type and operating conditions. Application to a representative resource and alternative turbine types is required.

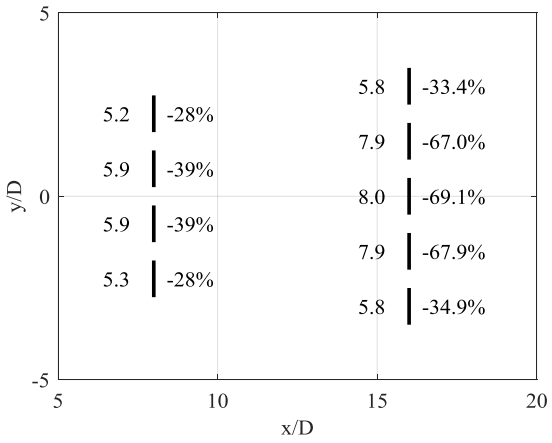

Figure 7: Left-hand-side variation of TSR, Right-hand-side variation in DEL from initial Row 1 at x/D = 0.

Author accepted manuscript of:
Mullings, H., Stallard, T. (2018) Unsteady Loading in a tidal array due to simulated turbulent onset flow. Paper Number 84. Proceedings of the 3rd International Conference on Renewable Energies Offshore. Lisbon, Portugal, 8-10 October 2018.

5 CONCLUSIONS

This study addresses the influence of onset turbulence and the presence of one- and multiple upstream wakes on unsteady loading and the resultant damage equivalent load (DEL) of tidal turbines. To apply a consistent approach to a range of sea-states and turbine array configurations a simplified load-spectrum model is employed based on blade element theory within a synthesised unsteady velocity field. A Synthetic Eddy Method and a von Kármán method provide similar turbulence intensity and length scale but result in a different spectrum of blade load. Over much of the frequency range the von Karman method provides reasonable prediction of the measured root bending moment spectrum, although this over-predicts the magnitude of fluctuations at high frequencies. The magnitude of a damage equivalent load at the rotor frequency by each method differs by around 15% with closer agreement with experiment by the von Kármán method.

Variation of damage equivalent load is examined due to an upstream turbine wake and for various locations within a small array. For a single downstream rotor, the resultant damage equivalent loads are reduced from the isolated rotor case for a partially offset rotor, 12% less, and reach a minimum for a turbine aligned with the upstream wake, 28% less. For a small multi-row array the reduction of damage equivalent load is larger, up to 40% on the second row and 57% for the central rotors on a third row. Such variations of DEL would result in differing design life of components and it is shown that similar damage equivalent loads may be attained for each turbine within an array by appropriate selection of the operating point of each turbine. For the turbine considered this approach also slightly increases power output from the array relative to the baseline case. This approach is thus promising for developing operating strategies for turbine arrays that balance turbine design life with array power output and a next step is to addresses the variation of operating point required throughout a tidal cycle. The approach to prediction of unsteady loading is simplified for this purpose and is being further developed to include variation of turbulence parameters across the wake region and the effect of waves.

6 ACKNOWLEDGEMENTS

The authors appreciate the support of EPSRC through DTP studentship (EP/P117127) and project X-MED (EP/J010235/1). DNV-GL also provided a research license for the use of Tidal Bladed, used here for turbulent flow synthesis.

7 REFERENCES

Ahmed, U., Apsley, D., Afghan, I., Stallard, T., and Stansby P.K. (2017). Fluctuating Loads on a Tidal Turbine Due to Velocity Shear and Turbulence: Comparison of CFD with Field Data. *Renewable Energy* 112(C), 235-246.

Blackmore, T., Myers, L. E., and Bahaj, A. S. (2016). Effects of turbulence on tidal turbines: Implications to performance, blade loads, and condition monitoring. *International Journal of Marine Energy* 14,1–26.

Bossanyi, E. (2003). GH Bladed User Manual. *Garrad Hassan and Partners Ltd*. Issue 11.

Burton, T., Sharpe, D., Jenkins, N., and Bossanyi, E. (2011). Wind energy Handbook. *Wiley Publishers*.

Carlier, C., Pinon, G., Gaurier, B., Germain, G. and Rivoalen, E. (2015), A Synthetic-Eddy-Method to represent the ambient turbulence in numerical simulation of marine current turbine. *In Proc. 11th EWTEC.*

Chamorro L. P., Hill C., Morton, S., C. Ellis, R. E. a. Arndt, and F. Sotiropoulos, (2013) On the interaction between a turbulent open channel flow and an axial-flow turbine, *Journal of Fluid Mechanics* 716, 658–670.

Cooke, S., Willden, R., Byrne B. Stallard, T and Olczak, A. (2015), Experimental Investigation of Thrust and Power on a Partial Array of tidal turbines. *In Proc. 11th EWTEC.*

Downing, S. D., Socie, D. F. (1982) Simple Rainflow counting Algorithms. *Int. Journal of Fatigue* 4(1), 31-40.

DNV-GL (2015). Standard Tidal Turbines (DNVGL-ST-0164).

Freebury, G. and Musial, W. (2000). Determining equivalent damage loading for fullscale wind turbine blade fatigue tests. *ASME Wind Energy Symposium.*

Galloway, P. (2013). Performance quantification of tidal turbines subjected to dynamic loading. *PhD Thesis*, University of Southampton.

Jarrin, N., Benhamadouche, S., Laurence, D., and Prosser, R. (2006). A synthetic-eddy method for generating inflow conditions for large-eddy simulations. *International Journal of Heat and Fluid Flow* 27(4), 585–593.

Author accepted manuscript of:
Mullings, H., Stallard, T. (2018) Unsteady Loading in a tidal array due to simulated turbulent onset flow. Paper Number 84. Proceedings of the 3rd International Conference on Renewable Energies Offshore. Lisbon, Portugal, 8-10 October 2018.

Lewis, M., Neill, S., Robins, P., Ward, P., Piano, M. and Hashemi, R. (2015). Observations of Flow Characteristics at Potential Tidal-Stream Energy Sites. *In Proc. 11th EWTEC*.

Mason-Jones, A., O'Doherty, D. and Morris, C. (2013), Influence of a velocity profile & support structure on tidal stream turbine performance. *Renewable Energy* 52, 23-30.

Masters, P., Chapman, J. and Willis M. (2011) A robust Blade Element Momentum Theory model for tidal stream turbines including tip and hub loss corrections. *Journal of Marine Engineering and Technology* 10, 25-35.

McCann, G. (2007) Tidal current turbine fatigue loading sensitivity to waves and turbulence – a parametric study. *In Proc. 7th EWTEC*.

Milne, I. A., Sharma, R. N., Flay R. G. J. and Bickerton, S. (2010) The Role of Onset Turbulence on Tidal Turbine Blade Loads, *17th Australasian Fluid Mechanics Conference*, Auckland New Zealand 59, 1–8.

Mullings, H., Stallard, T. and Payne, G. (2017) Operational Loads on a Tidal Turbine due to Environmental Conditions, *In Proc. 27th ISOPE*.

Mycek, P., Gaurier, B., Germain, G., Pinon, G. and E. Rivoalen, (2014) Experimental study of the turbulence intensity effects on marine current turbines behaviour. Part I: One single turbine, *Renewable Energy* 66, 729–746.

Olczak, A., Stallard, T., Feng, T. and Stansby, P. (2016), Hydrodynamic loadings on a horizontal axis tidal turbine prototype. *Journal of Fluids and Structures*, 71: 78-95.

Ouro, P., Harrold, M. and Stoesser T. (2017), Comparison of a RANS blade element model for tidal turbine arrays with laboratory scale measurements of wake velocity and rotor thrust. *Journal of Fluids and Structures*, 64: 87-106.

Payne, G. S., Stallard, T., and Martinez, R. (2017a). Design and manufacture of a bed supported tidal turbine model for blade and shaft load measurement in turbulent flow and waves. *Renewable Energy*, 107:312–326.

Payne, G. S., Stallard, T., Mullings, H. and Martinez, R. (2017b). Experimental Investigation into Unsteady Loads on Horizontal Axis Tidal Turbines. *In Proc. 12th EWTEC*.

Poletto, R., Craft, T., and Revell, A. (2013), A new divergence free synthetic eddy method for the reproduction of inlet flow conditions for LES. *Journal of Flow, Turbulence and Combustion*, 91(3): 519-539.

Smilden, E., Sørensen, A., and Eliassen, L. (2016). Wind model for simulation of thrust variations on a wind turbine. *Energy Procedia*, 94: 306-318.

Stallard T., Collings, R., Feng, T. and Whelan, J. (2013), Interactions between tidal turbine wakes: experimental study of a group of three-bladed rotors. *Phil Trans R Soc A* 371: 20120159.

Stallard T., Feng, T. and Stansby, P. (2015), Experimental study of the mean wake of a tidal stream rotor in a shallow turbulent flow. *Journal of Fluids and Structures* 54, 234-46.

Stansby, P. and Stallard T. (2016), Fast optimization of tidal stream turbine positions for power generation in small arrays with low blockage based on superposition of self-similar far-wake velocity deficit profiles. *Renewable Energy*, 92: 366-375.

Togneri, M. Masters, I. and Orme, J. (2011) Incorporating Turbulent Inflow Conditions in a Blade Element Momentum Model of Tidal Stream Turbines. *In Proc*. 21st *ISOPE*.

Togneri, M., Masters, I., Carlier, C., Choma Bex, C, Pinon, G. (2017) Comparison of synthetic turbulence approaches for two numerical tidal turbine models. *In Proc. 12th EWTEC*.

Vogel, C., and Willden, R. (2017), Multi-Rotor Tidal Stream Turbine Fence performance and operation. *International Journal of Marine Energy* 19, 198-206.